University of Warsaw
Faculty of Physics

Agnieszka Wierzbicka
Student's book no.: 323371

Analysis of laminar profile of evoked potentials in rat visual cortex

Master's degree thesis
field of study Applications of Physics in Biology and Medicine
speciality Neuroinformatics

The thesis written under the supervision of
Jarosław Żygierewicz, Ph.D.
Biomedical Physics Division
Instytute of Experimental Physics
Faculty of Physics, University of Warsaw
and
prof. Wioletta Waleszczyk
Laboratory of Visual Neurobiology
Department of Neurophysiology
Nencki Institute of Experimental Biology PAS

Warsaw, December 2017

Oświadczenie kierującego pracą

Oświadczam, że niniejsza praca została przygotowana pod moim kierunkiem i stwierdzam, że spełnia ona warunki do przedstawienia jej w postępowaniu o nadanie tytułu zawodowego.

Data Podpis kierującego pracą

Statement of the Supervisor on Submission of the Thesis

I hereby certify that the thesis submitted has been prepared under my supervision and I declare that it satisfies the requirements of submission in the proceedings for the award of a degree.

Date Signature of the Supervisor

Oświadczenie autora (autorów) pracy

Świadom odpowiedzialności prawnej oświadczam, że niniejsza praca dyplomowa została napisana przeze mnie samodzielnie i nie zawiera treści uzyskanych w sposób niezgodny z obowiązującymi przepisami.

Oświadczam również, że przedstawiona praca nie była wcześniej przedmiotem procedur związanych z uzyskaniem tytułu zawodowego w wyższej uczelni.

Oświadczam ponadto, że niniejsza wersja pracy jest identyczna z załączoną wersją elektroniczną.

Data Podpis autora (autorów) pracy

Statement of the Author(s) on Submission of the Thesis

Aware of legal liability I certify that the thesis submitted has been prepared by myself and does not include information gathered contrary to the law.

I also declare that the thesis submitted has not been the subject of proceedings resulting in the award of a university degree.

Furthermore I certify that the submitted version of the thesis is identical with its attached electronic version.

Date Signature of the Author(s) of the thesis

Summary

Key words

electrophysiology, visual system, primary visual cortex, visual stimulation, local field potential, current source density, temporal frequency
elektrofizjologia, układ wzrokowy, pierwszorzędowa kora wzrokowa, stymulacja wzrokowa, lokalny potencjał polowy, current source density, częstotliwość czasowa
po polsku czy po ang?

Area of study (codes according to Erasmus Subject Area Codes List)

13.2 Physics

The title of the thesis in Polish

Analiza profilu warstowego potencjałów wywołanych w korze wzrokowej szczura

Table of contents

Goal . . . 3

1. Introduction . . . 4
1.1. Structure of the visual system . . . 4
1.2. Parallel processing in the visual system . . . 4
1.3. Architecture of primary visual cortex . . . 5
1.4. Local field potential . . . 6

2. Materials and methods . . . 8
2.1. Subjects . . . 8
2.2. Surgical procedures . . . 8
2.3. Stimulation electrode . . . 8
2.4. Stimulation procedure . . . 10

3. Data analysis . . . 11
3.1. Data preparation . . . 11
3.2. Averaging visual potentials . . . 12
3.2.1. Description of the method . . . 12
3.2.2. Measurement of peak amplitude in VEP . . . 13
3.3. Estimation of signal spectrum . . . 14
3.4. Current Source Density . . . 15

4. Results . . . 17
4.1. Overview of results obtain in the time domain . . . 17
4.2. Overview of results obtain in the frequency domain . . . 20
4.3. Analysis of current source density . . . 22
4.4. Analysis of laminar profile for stimulation with 1 Hz frequency . . . 23
4.5. Laminar analysis for stimulation with 2 Hz frequency . . . 25
4.6. Laminar analysis for stimulation with 4 Hz frequency . . . 26
4.7. Laminar analysis for stimulation with 7 Hz frequency . . . 26
4.8. Laminar analysis for stimulation with 10 Hz frequency . . . 27
4.9. Laminar analysis for stimulation with 12 Hz frequency . . . 27

5. Discussion . . . 28

Bibliography . . . 29

Goal

The main goal of this work was to study responses of neurons from particular layers of visual cortex to visual stimulation with different temporal frequency.

Chapter 1

Introduction

1.1. Structure of the visual system

Visual perception is an ability to process information coded by light. There are two largely independent visual pathways. Both begin in retina where light is converted into electrical discharge by photoreceptors and then thew information is transferred to ganglion cells and then further via the optic nerve (Fig. 1.1). Here the pathways split. The first one, known as geniculate visual pathway, leads via the dorsal part of lateral geniculate nucleus (LGN) to primary visual cortex (VCx), and from there further to higher-order cortex. The second pathway, known as extrageniculate visual pathway, leads through superior colliculus and the lateral posterior nucleus-pulvinar complex and then—similarly to the first pathway—reaches primary visual cortex and the higher-order cortex.(Waleszczyk et al., 2005, Thomson, 2010).

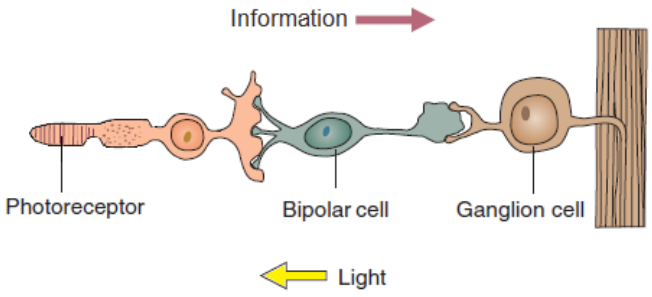

Figure 1.1: Neural circuitry in the retina (modified from Carlson, 2013).

1.2. Parallel processing in the visual system

Retina is the first place where visual information is decoded and segregated. Three main morphological types of ganglion cells recognize different properties of visual stimuli (Fig. 1.2).

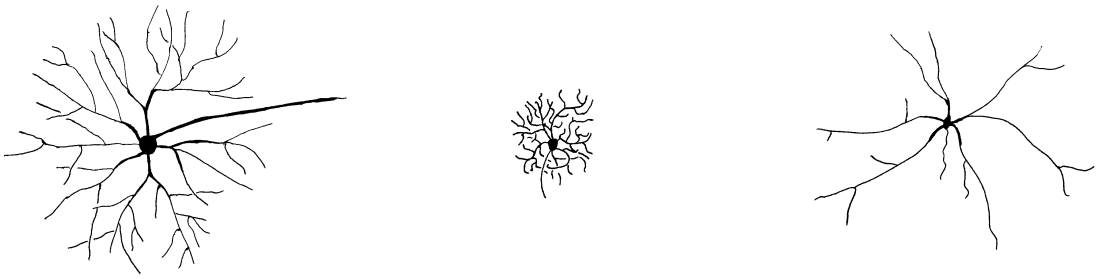

(a) Magnocellular (b) Parvocellular (c) Koniocellular

Figure 1.2: Three most important morphological classes of ganglion cells (Drawing on the basis of Stone, 1983).

Magnocellular cells (Fig. 1.2a) have big soma with large dendritic tree. Thanks to lthick axon this type of cells can recognize fast stimuli but have poor spatial frequency. Parvocellular cells are cells with medium soma (Fig. 1.2b). They are characterized by high resolution spatial frequency due to small dendritic size, but weak temporal frequency resolution. Koniocellular cells are heterogeneous group of cells with small-to-medium somata of different dendritic morphologies (Fig. 1.2c; Stone, 1983, Waleszczyk et al., 2005).

1.3. Architecture of primary visual cortex

Primary visual cortex can be divided into 6 vertical layers differing from one another in function and morphology. Sometimes layers II and III are considered to be one layer II/III (Fig. 1.3). (Waleszczyk et al., 2005)

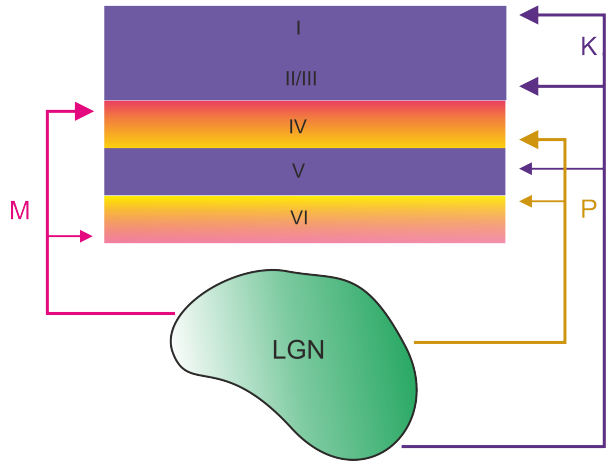

Figure 1.3: The main connections made by axons from the dorsal lateral geniculate body to primary visual cortex.

First main division is made based on granule cells located in layer IV. These cells are characterized by very small cell bodies. Layers above IV are called *supragranular* while layers below are referred to as *infragranular*. As it was shown (by Maier et al., 2010), around layer IV there is a polarization change observable on averaged evoked potentials chart. In layer I cell bodies are absent but there are plenty of axons, dendrites, and synapses. Two major

classes of cortical cells are pyramidal cells which occur in all layers except I and IV, and stellate cells which are found in all layers (Fig. 1.4).

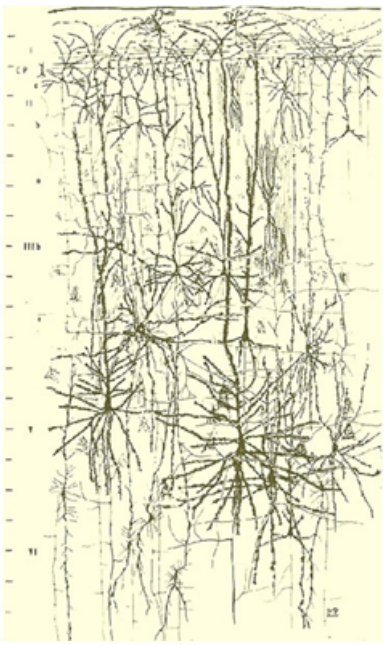

Figure 1.4: Composite figure of a mosaic of camera lucida drawings showing the morphological features (size, location, and distribution) of the principal neuronal types of the human cortex. From rapid-Golgi preparations. Scale (on the left): 100 μm (Schmolesky, 2007).

1.4. Local field potential

Electrophysiology is a method to record activity of the brain with high temporal resolution and weaker spatial. Thanks to electrodes inserted in different places the brain we can gather information from them. It can be used to check the response for various stimuli at different locations. Usage of vertical electrodes allows to record simultaneously signal across the brain. Nearly all visual information enters the cortex via area VCx.

Local field potentials (LFP), the low-frequency part of extracellular electrical recordings from electrodes inserted into the examined tissue, are a measure of the neural activity reflecting dendritic processing of synaptic inputs to neuronal populations. LFP is a superposition of postsynaptic and action potentials (Fig. 1.5).

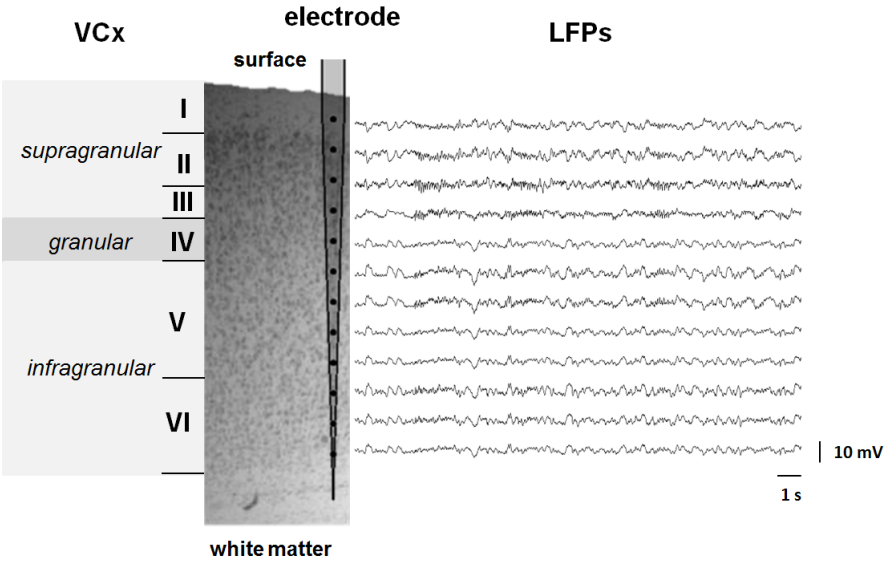

Figure 1.5: An example of LFP signals recorded in VCx.

Postsynaptic potentials are potentials that are generated in the postsynaptic membrane of a dendrite of nerve cell. They can be either excitatory (Excitatory Post-Synaptic Potentials, EPSPs)—that enhance chance of induces action potentials or inhibitory (Inhibitory Post-Synaptic Potentials, IPSPs)—making action potential less likely to happen. Lots of potentials reach neuron. When the sum of them reaches a threshold the neuron becomes excited and generates an action potential which propagates along axon (Fig. 1.6).

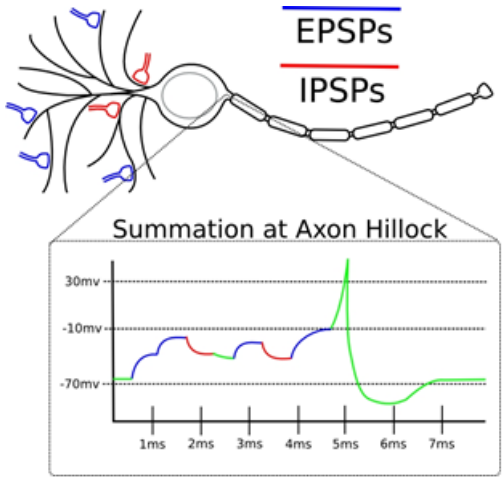

Figure 1.6: Excitatory and inhibitory post-synaptic potentials.

Chapter 2

Materials and methods

2.1. Subjects

For electrophysiological experiments presented in this study, we used 6 adult male Wistar rats (250-300g). All animals were housed with free access to food and water and maintained on a 12 h light/dark cycle. All experimental procedures were conducted in accordance with the ARVO Statement for the Use of Animals in Ophthalmic and Vision Research and the EC Directive 86/609/EEC for animal experiments using protocols and methods accepted by the First Warsaw Local Ethical Commission for Animal Experimentation. The experiments took place in Laboratory of Visual Neurobiology in Nencki Institute with great help from mgr Katarzyna Kordecka.

2.2. Surgical procedures

Animals under deep urethane anesthesia (1.5 g/kg, Sigma-Aldrich, Germany, 30% aqueous solution, i.p) were placed in a stereotaxic apparatus. Additional doses of urethane (0.15 g/kg) were administered when necessary. Body temperature was maintained between 36 and 38 °C using an automatically controlled electric heating blanket. Every hour fluid requirements were fulfilled by subcutaneous injections of 0.9% NaCl (1ml/hour) and eyes were humidified with Vidisic (Polfa Warszawa S.A., Poland) to prevent cornea from drying. The skin on the head was disinfected with iodine and local anesthetic with 1% lidocaine hydrochloride (0.5 ml, Polfa Warszawa S.A., Poland) was injected over the scalp. The skull was opened to expose areas of the binocular primary VCx (7.5 mm posterior to bregma, 5.0 mm lateral) in left hemisphere. Coordinates of electrode were chosen based on the rat brain atlas of Paxinos and Watson (Paxinos and Watson, 2007).

2.3. Stimulation electrode

For all experiments the same custom vertical and made of tungsten electrode was used (Fig. 2.1). The contacts on the electrode were chosen based on previous experiments when it turned out that it is difficult to record precisely from layer IV which is very thin and (i w dodatku można w niej zaobserować repolaryzację w sensie jest dużo kanałów z dodatnim i ujemnym potencjałem a samo przegięcie występuje tylko na jednej głębokości. w zależności właśnie od tego miejsca wyznaczano głębokość warstwy IV i resztę kanałów dopasowywano względem niej.)

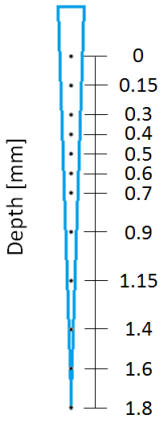

Figure 2.1: Scheme of 12-channel vertical electrode with intervals between contacts expressed in mm.

Chociaż użyto tej samej elektrody do wszystkich doświadczeń to nie zawsze te same kanały odpowiadały tym samym głębokością, co wynika z różnic anatomicznych między zwierzętami a także metodą która nie jest bardzo dokładna przestrzennie i nawet na tej samej głębokości może rejestrować sygnał pochodzący z miejsca ciut wyżej lub niżej niż u innego zwierzaka. In Table 2.1 podsumowano które kanały zostały uwzględnione dla wszystkich zwierzaków.

Table 2.1: Summary of all channels that have been used for each animal.

Depth [mm]	**Rat1**	**Rat2**	**Rat3**	**Rat4**	**Rat5**	**Rat6**
0	1	1	1	1	1	1
0.15			2		2	
0.3	2	2		2		2
0.4			3			
0.5	3	3	4	3	3	3
0.6		4		4		4
0.7	4				4	
0.9		5	5	5	5	5
1.15	5				6	6
1.4		6	6	6	7	
1.6	6					7
1.8	7	7	7	7		

2.4. Stimulation procedure

In the experiments stimuli were presented with interstimulus intervals of 1, 0.5, 0.25, 0.2, 0.143, 0.08 [s] which correspond to frequencies 1, 2, 4, 7, 10, 12 [Hz], respectively. An individual stimulus was a 2-millisecond-long LED flash at 560 cd/m^2 luminance. It was dark in the room and rats had both eyes opened. For each frequency the stimuli were applied in 40 repetitions of 5-second-long series with random (2-3 s) breaks between them (Fig. 2.2).

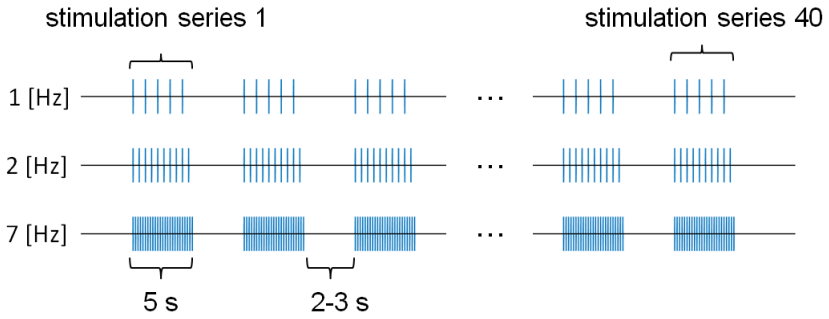

Figure 2.2: Stimulation protocol. The stimuli were presented in 5 s long 40 series at given frequency (from 1 to 12 Hz). The number of stimuli in a series depends on frequency.

Chapter 3

Data analysis

3.1. Data preparation

Signal was filtered bandpass in range of 0.3-500 Hz with 500 gain using differential AC amplifiers (A-M 140 Systems, US) and recorded with sampling frequency 1000 Hz. For further analysis hardware filter turned out to not be enough so three other, Butterworth filters was used: 1^{st} order lowpass at cut off 100 Hz, 1^{st} order bandstop at cut off between 45 and 55 Hz and 1^{st} order highpass at cut off 0.5 Hz. To avoid change of phase of the signal *filtfilt* function was used. After filtering each channels of data was normalized by subtracting the mean of all recording for each channel and divided by their standard deviation. Butterworth filters was used because they are characterized by low deformation of signal giving smooth and monotonic transfer function. It is at cost of low efficiency of filtering, but for this data it was sufficient. After this preparation data was cut into 6-s-long chunks from -0.5 s to 5.5 s where 0 was the beginning of stimulation and averaged across trials. For further analysis 7 channels out of 12 from contralateral (in respect of stimulation side) VCx were chosen to obtain representative profile: 3 of supragranular, 3 of infragranular and one channel from granular layer (layer IV; Fig 3.1).

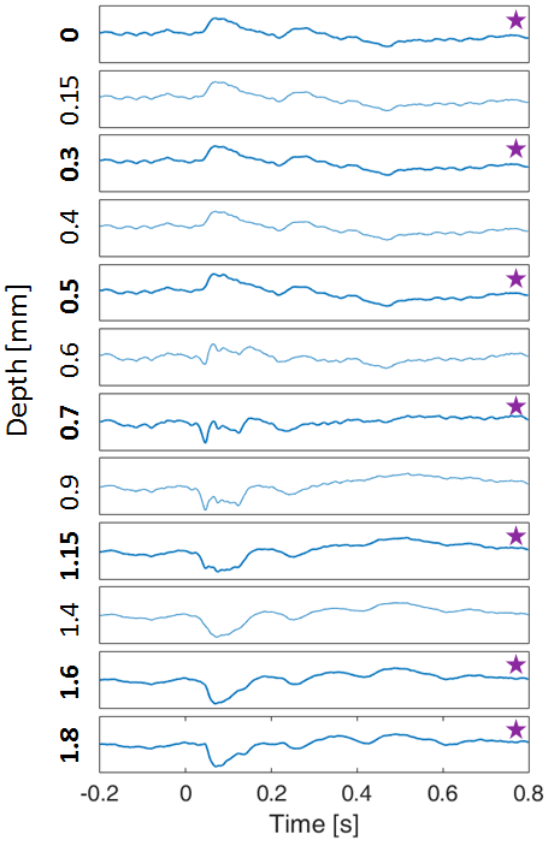

Figure 3.1: Averaged evoked potentials from VCx from Rat1. On channels at 0.6 and 0.7 mm depth repolarization can be observed. Channels chosen to further analysis are marked by purple stars. Time 0 s means an occurrence of stimulus. Y axis the same for all subfigures.

Reduction of number of channels was necessary due to two reasons:

- sometimes short circuits between channels occurred
- there were differences of depth of electrodes and layer IV was recorded by different channels

The choice was made based of analysis on the averaged evoked potentials. The reference of depth was channel with repolarization just after a stimulus occurred and treated as from layer IV, then 3 shallower channels and 3 deeper channels with increasing amplitude.

3.2. Averaging visual potentials

3.2.1. Description of the method

Visual Evoked Potential (VEP) is a case of steady state evoked potential where light is a stimulus. In theory spontaneous activity of ECoG is a stochastic process (independent, stationary noise with mean equal to zero) and brain response to each stimulus is constant.

In that way signal in each realization can be expressed by

$$x_i(t) = s(t) + n_i(t), \tag{3.1}$$

where $s(t)$ is a real signal, $n_i(t)$ noise part. For white noise with mean zero, expected value equals:

$$E\left[\frac{1}{N}\sum_{i=1}^{N} n_i(t)\right] = 0, \tag{3.2}$$

which causes that for averaged signal: $E\left[\bar{x}(t)\right] = s(t)$.

The effect of averaging is shown on Figure 3.2. Visual response to a single visual stimulus is usually too weak to distinguish from the background of spontaneous activity of visual cortex. Averaging across several repetitions makes evoked potential stand out.

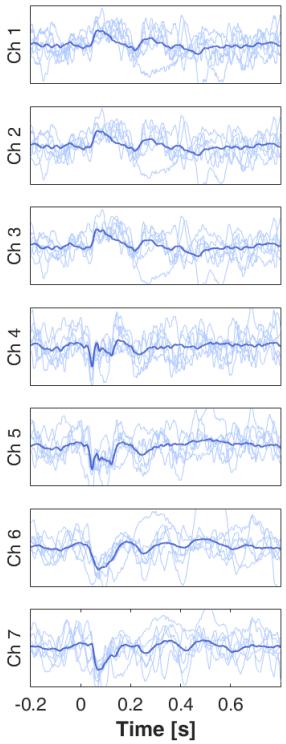

Figure 3.2: Comparison between single trials and their average for Rat1. Lighter blue lines represent few examples of responses to a single repetition of a stimulus. Bold and darker line is the averaged across all trials. Y axis is the same for all subfigures.

3.2.2. Measurement of peak amplitude in VEP

For stimulation with frequencies 1 and 2 Hz it was possible to observe visual evoked potentials. There were always two deflections from zero: first almost immediately and second around 0.3 s after a stimulus (Fig. 3.3). Further they are called first and second peak (no matter whether they are negative or positive).

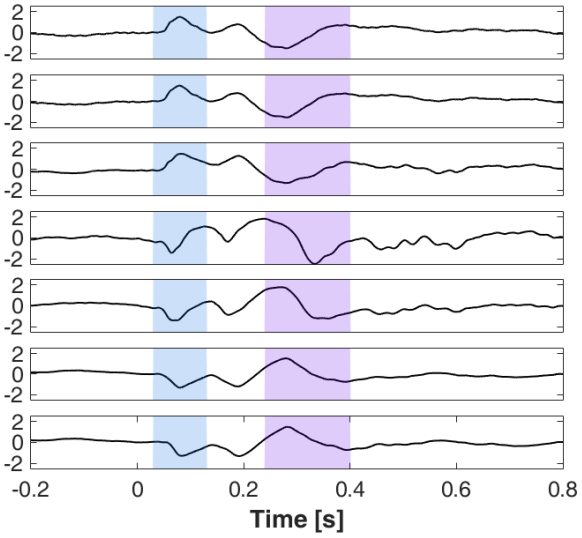

Figure 3.3: Averaged potentials for Rat4 with stimulation with 1 Hz. Amplitude of the first peak was calculated for blue background (0.03 - 0.13 s after stimulus). Amplitude of the second peak was calculated for purple background (0.24 - 0.4 s after stimulus).

On Figure 3.4 first channel for the same rat as on Figure 3.3 is presented. An amplitude was taken to be the most extreme value (i.e. having the highest absolute value) in a specified time after an occurrence of a stimulus.

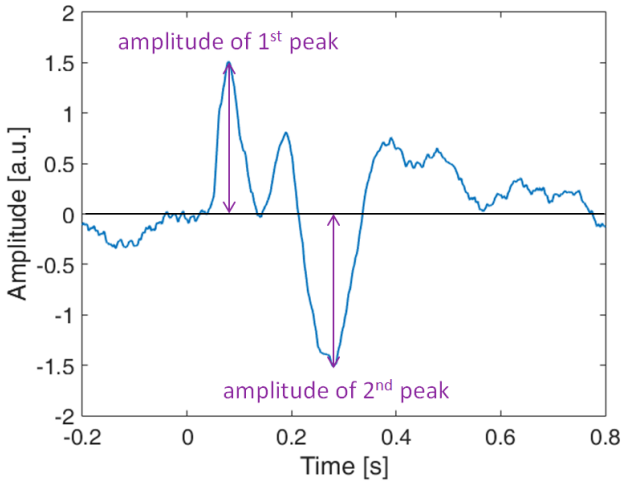

Figure 3.4: Measurement of the peaks amplitude for channel 1 of Rat4 in stimulation with 1 Hz.

3.3. Estimation of signal spectrum

Spectra of the signals were estimated by the method, introduced by Welch (Welch, 1967). It relies on splitting the signal into overlapping time windows, estimation of the periodogram for each of the windows, and then averaging of the estimates. In this experiment, data was averaged by 5-second-long chunks for 7 channels and estimation of power spectrum density

was calculated. Hamming window with 3-second-long with overlap of 2 seconds was used. On Figure 3.5 measurement of the amplitude of fundamental frequency and second harmonic is presented. Amplitudes are the exact values of power spectrum in specific frequencies.

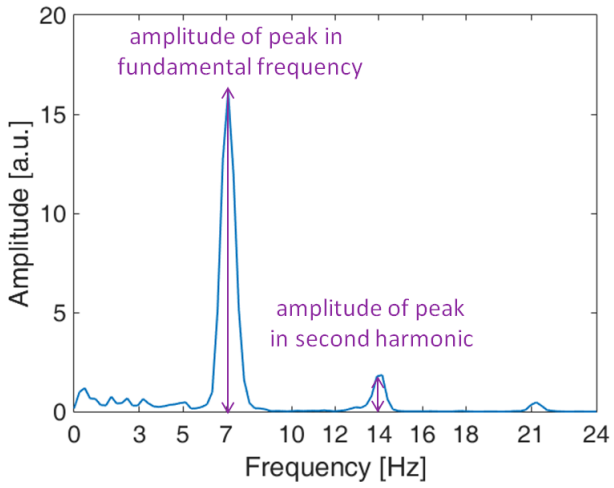

Figure 3.5: Measurement of the peak amplitude for channel 1 of Rat4 in stimulation with 7 Hz.

3.4. Current Source Density

To localize synaptic dynamics, it is convenient, whenever possible, to estimate the density of transmembrane current sources (CSD) generating the LFP. Let us assume that we record potential in infinitive, homogeneous ans isotropic conductive medium. Current I in that tissue has current density $\vec{J}$ given by equation:

$$\vec{J} = \frac{I\vec{r}}{4\pi r^2} \tag{3.3}$$

radially at a distance r from the source. In conductive medium with conductivity σ Ohm's law describes relation between current density and potential:

$$\vec{J} = -\sigma \nabla V. \tag{3.4}$$

Multitude of currents I_j located at $\vec{r_j}$ induce potential:

$$V(\vec{r}) = \sum_j \frac{I_j}{4\pi\sigma|\vec{r} - \vec{r'}|}. \tag{3.5}$$

Introducing current source density equals to:

$$C(\vec{r}) = \sum_j I_j \delta(\vec{r} - \vec{r'}), \tag{3.6}$$

we can find a relation between potential and CSD:

$$V(\vec{r}) = \frac{1}{4\pi\sigma} \int d^3\vec{r'} \frac{C(\vec{r'})}{|\vec{r} - \vec{r'}|}, \tag{3.7}$$

where V is potential generated by sources, σ is a conductivity, $\vec{r}$ is a distance between potential and source. By inverting this relation we get Poisson equation:

$$C(\vec{r}) = -\sigma \Delta V. \tag{3.8}$$

Equation 3.8 can be generalized for arbitrary conductivity tensor fields σ:

$$C(\vec{r}) = -\nabla \cdot [\sigma \nabla V]. \tag{3.9}$$

In this work to calculate CSD the method introduced by Jan Potworowski called *kernel Current Source Density* (kCSD) was used (Wójcik, 2014, Potworowski et al., 2012).

Chapter 4

Results

4.1. Overview of results obtain in the time domain

Next, there are all experiments with 6 different stimulation frequency presented one after another. In the Figure 4.1 results of stimulation with 1 and 2 Hz frequencies are presented—there is a clear peak of response after each repetition of stimulus.

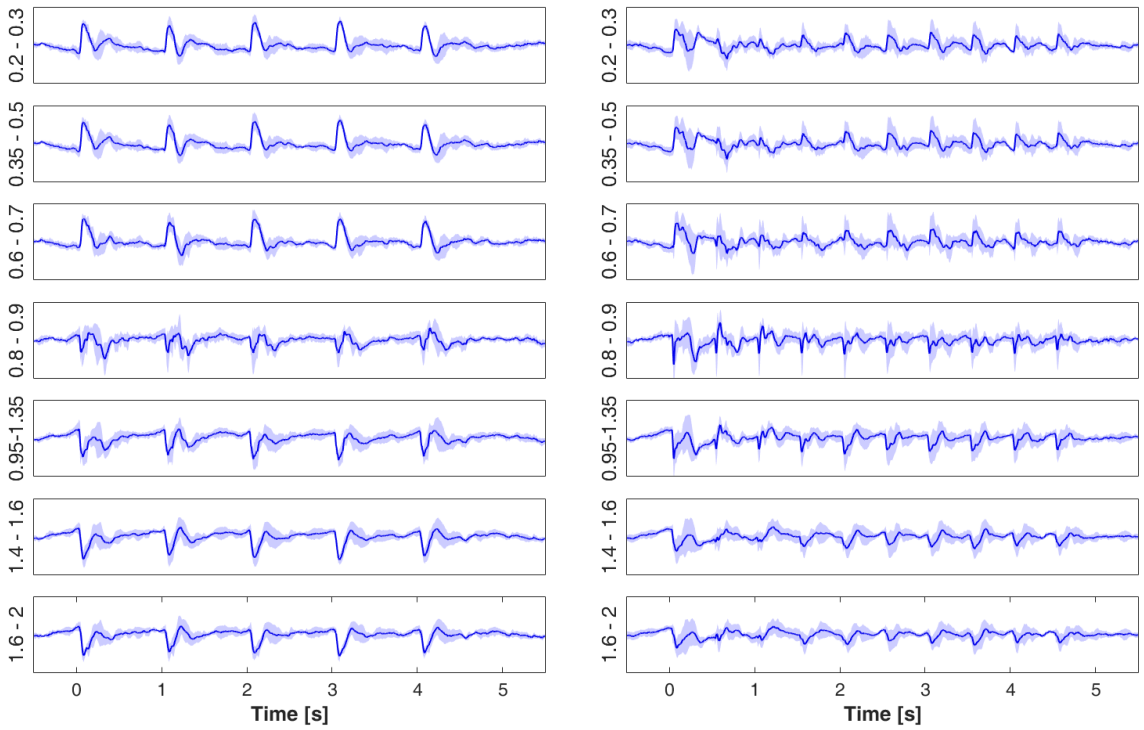

(a) Averaged signal for stimulation of 1 Hz.

(b) Averaged signal for stimulation of 2 Hz.

Figure 4.1: Averaged signal across 40 repetitions of stimuli.

For frequencies higher than 2 Hz signals look different (Fig. 4.2). Firstly the response for stimuli is blurred: stimuli occurs so often that it is impossible to determine where response for certain stimulus starts and ends. The signal forms a continuous oscillation. During the first 1.5 s of the stimulation: the amplitude of oscillations is higher than for the rest. At around

5.1 s there is noticeable peak probably as a response to end of stimulation.

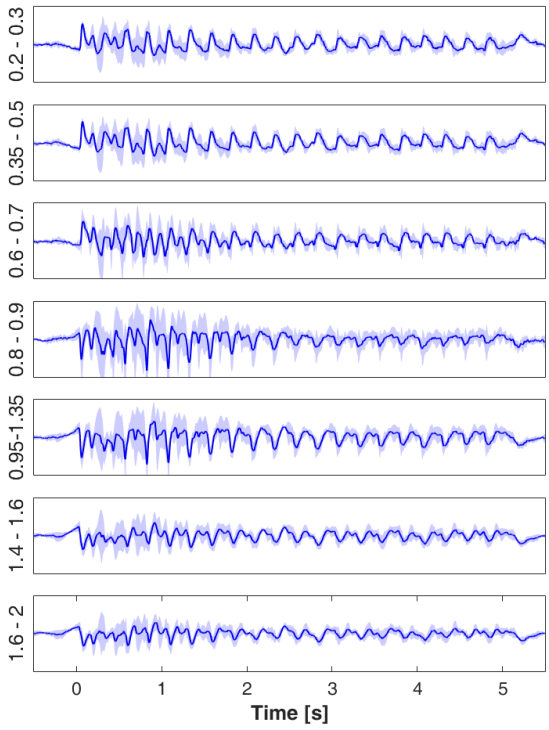

(a) Averaged signal for stimulation of 4 Hz.

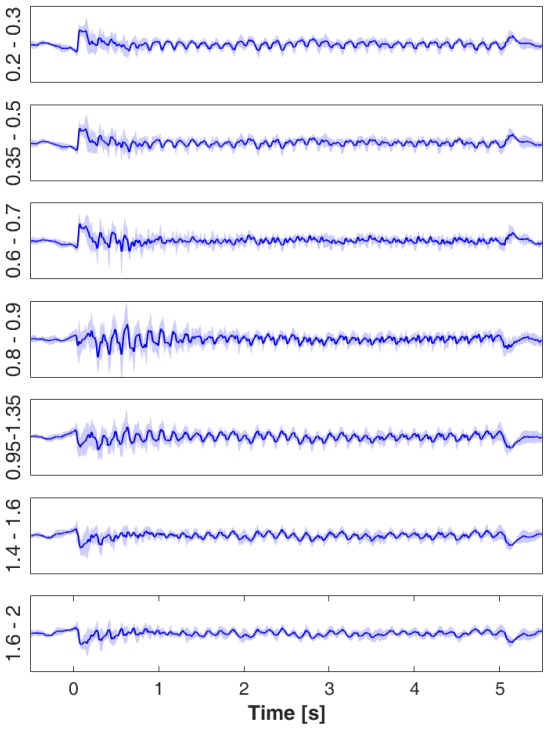

(b) Averaged signal for stimulation of 7 Hz.

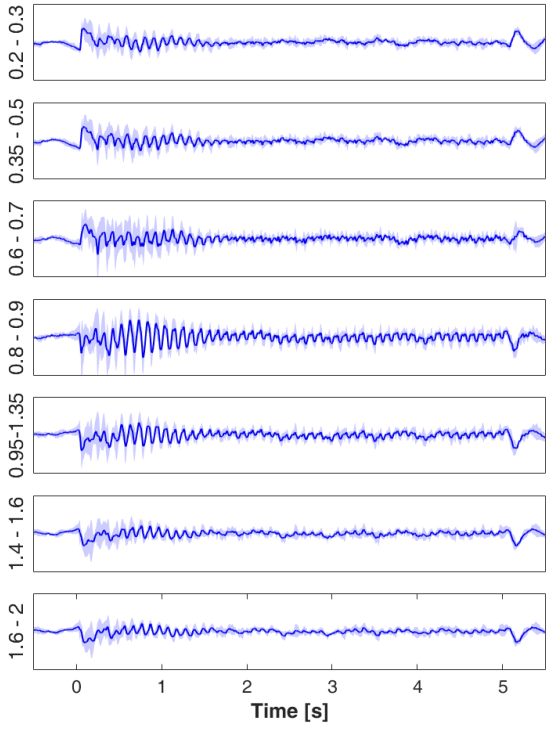

(c) Averaged signal for stimulation of 10 Hz.

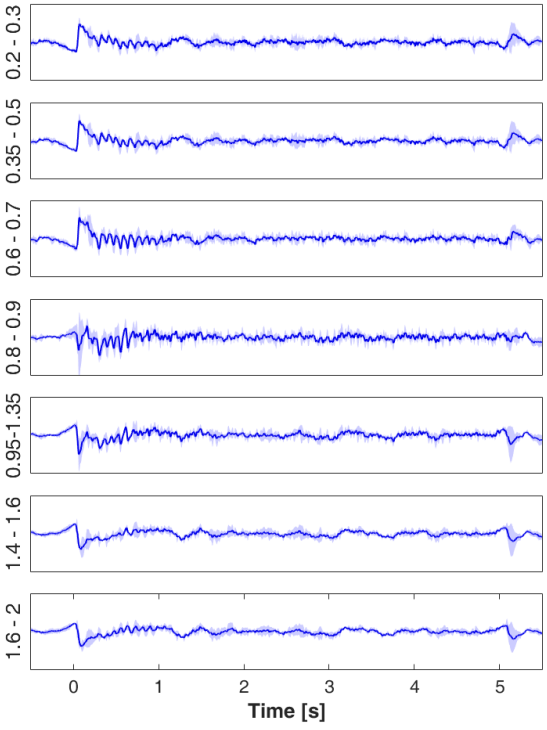

(d) Averaged signal for stimulation of 12 Hz.

Figure 4.2: All experiments averaged by 40 trials in time domain. Point 0 s shows beginning of 5 s constant stimulation. Blue intervals represent standard deviations by the animals. Y axis is the same for all subfigures.

4.2. Overview of results obtain in the frequency domain

Next, all power spectra calculated by Welch's methods are shown in Fig. 4.3. For stimulation of 1 Hz there are up to 5 harmonic, sometimes even bigger than the fundamental frequency (Fig. 4.3a). For frequencies 2 – 10 Hz, the fundamental frequency and the second harmonic are clean and much bigger than others (Fig. 4.3b – 4.3e). Response for 12 Hz in power spectrum is noticeably weaker – peak in the fundamental frequency is at the same level as low frequency noise (Fig. 4.3f).

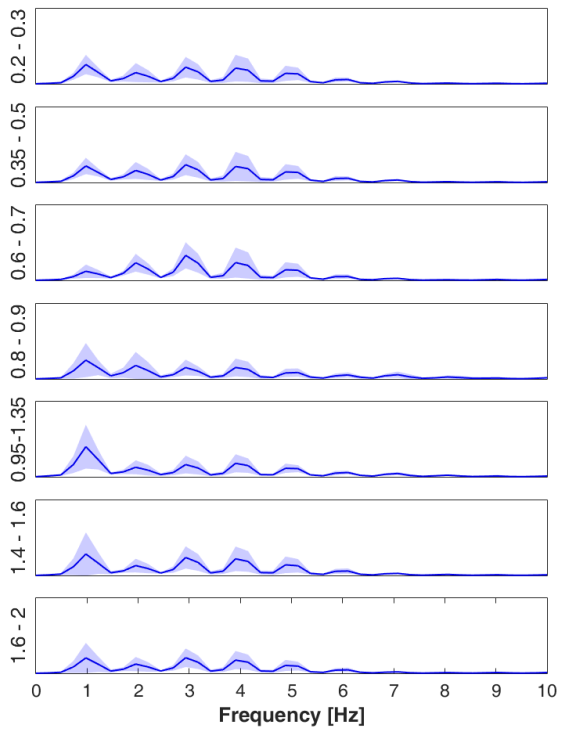

(a) Power spectrum for stimulation of 1 Hz.

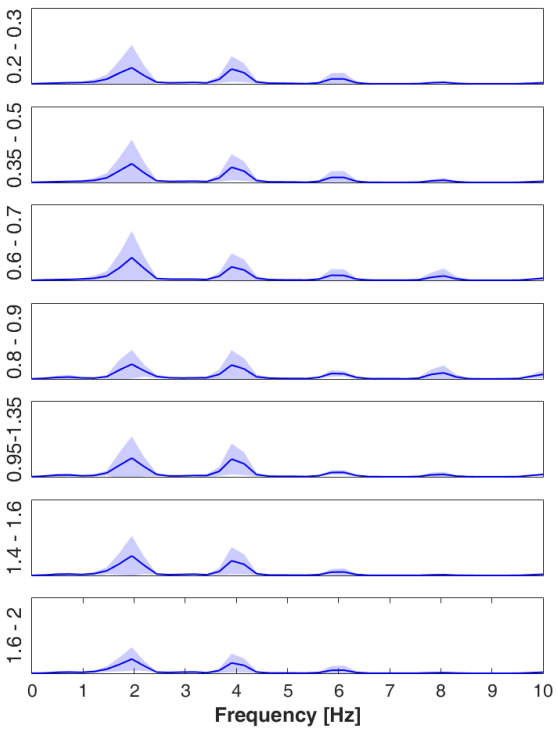

(b) Power spectrum for stimulation of 2 Hz.

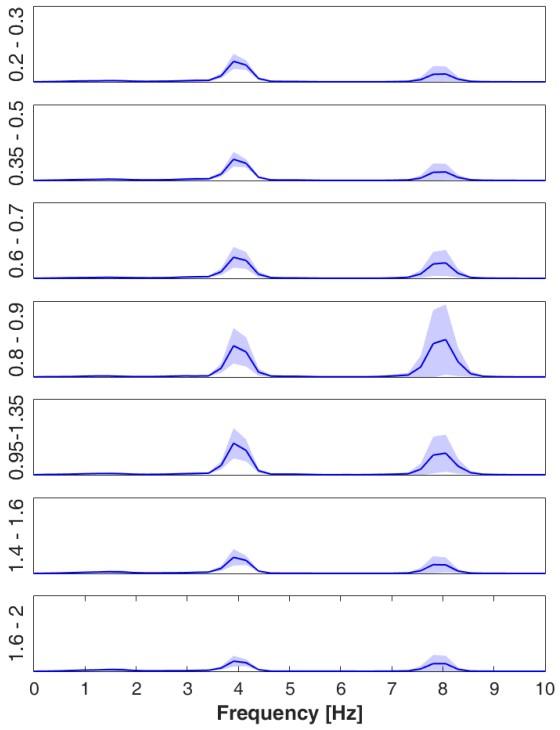

(c) Power spectrum for stimulation of 4 Hz.

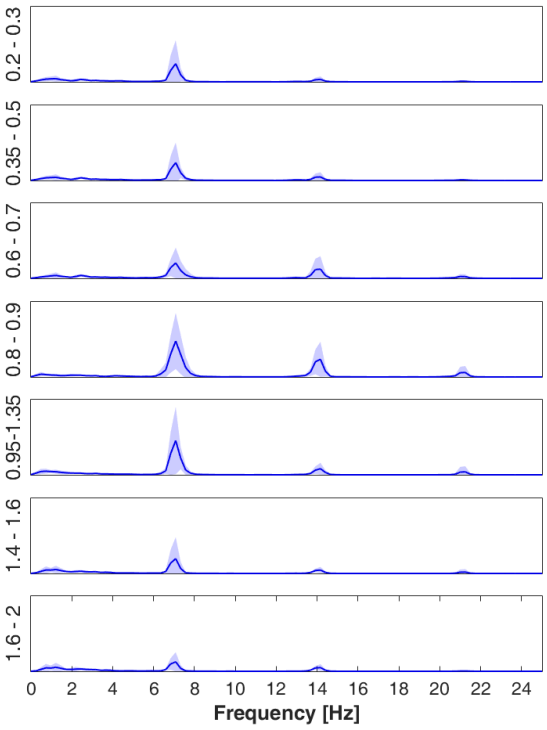

(d) Power spectrum for stimulation of 7 Hz.

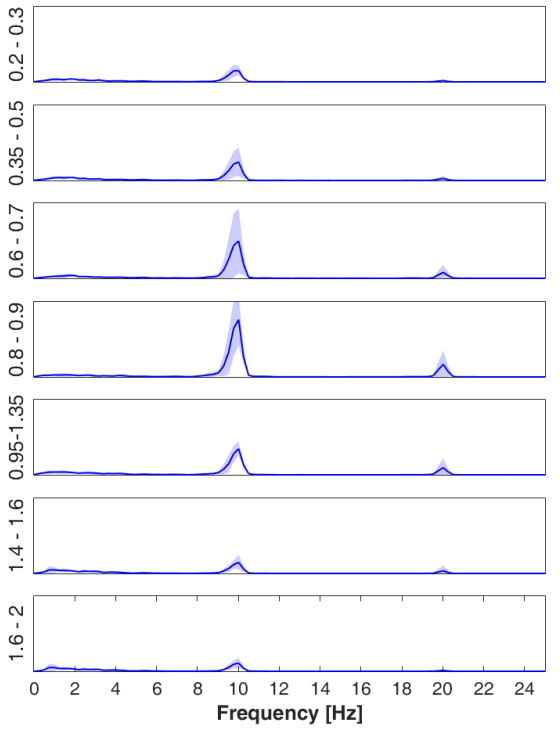

(e) Power spectrum for stimulation of 10 Hz.

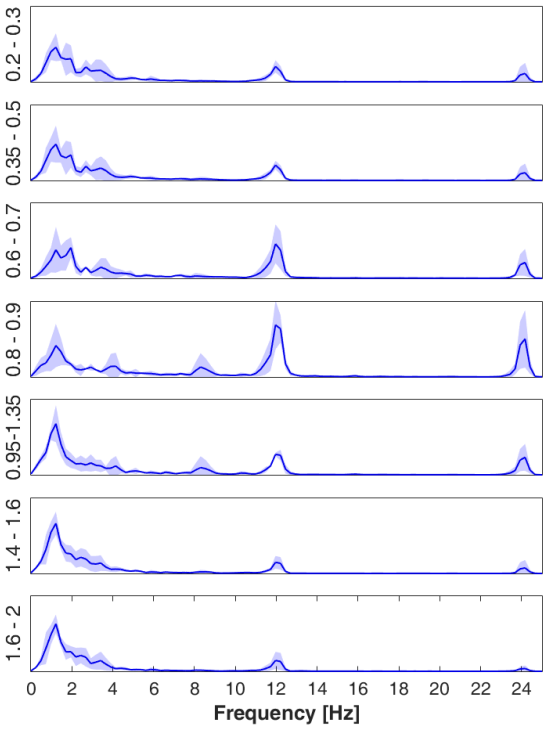

(f) Power spectrum for stimulation of 12 Hz.

Figure 4.3: Power spectrum calculated for average by 40 trials for each animal. Blue intervals represent standard deviations by the animals. Y axis is different for all subfigures.

4.3. Analysis of current source density

Current source density analysis is shown in Figure 4.4. For stimulation of 1 and 2 Hz there is a change in polarization to each repetition of stimulus. For stimulation of frequency higher than 2 Hz there is a change of polarization just after end of stimulation (around 5.1 s).

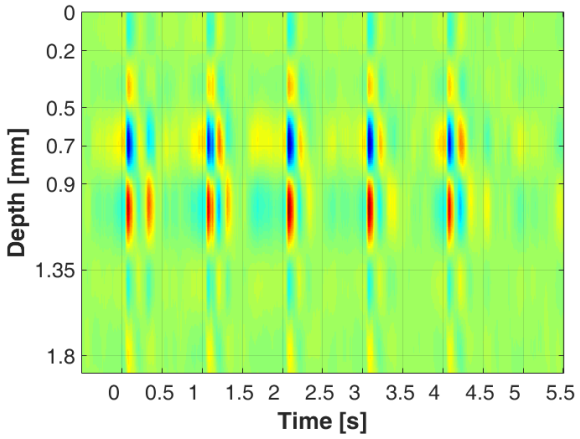

(a) CSD for stimulation of 1 Hz.

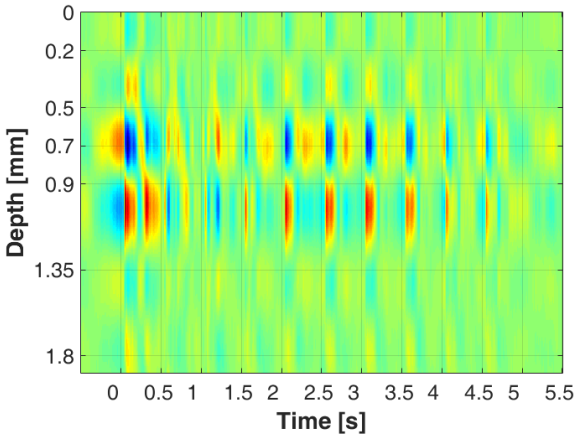

(b) CSD for stimulation of 2 Hz.

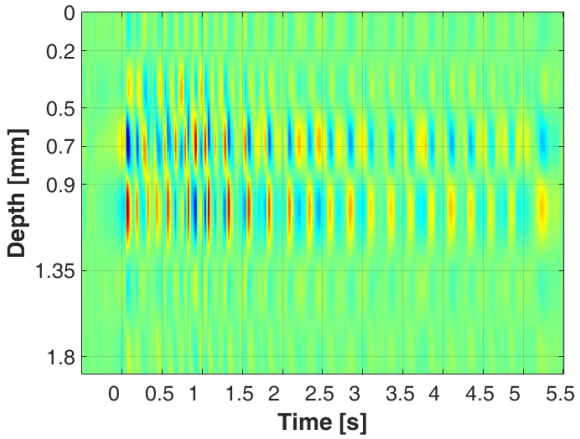

(c) CSD for stimulation of 4 Hz.

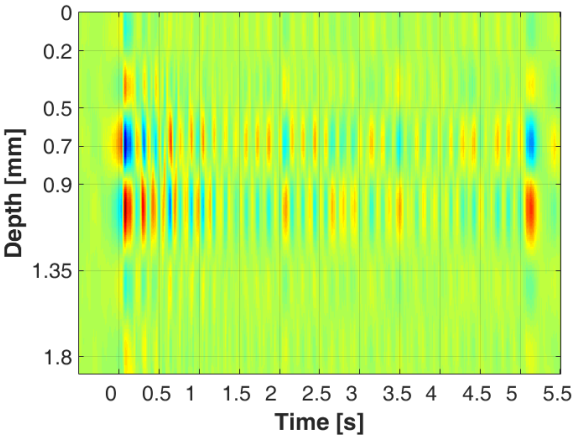

(d) CSD for stimulation of 7 Hz.

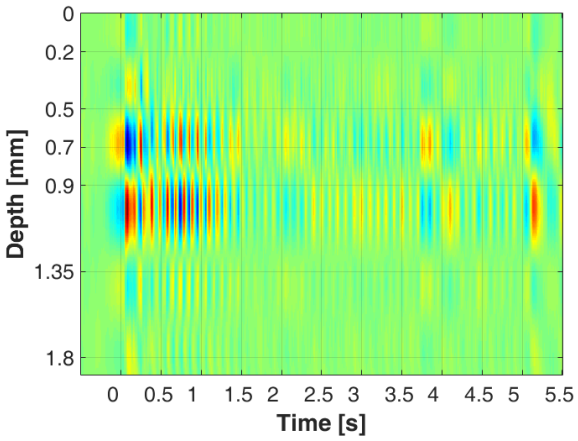

(e) CSD for stimulation of 10 Hz.

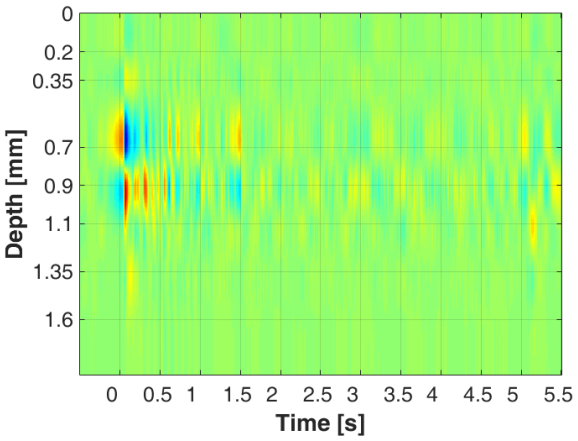

(f) CSD for stimulation of 12 Hz.

Figure 4.4: All experiments averaged by 40 trials and CSD is performed. Point 0 s shows beginning of 5 s constant stimulation. Scale is from blue (source) to red (sink). Y axis is the same for all subfigures.

4.4. Analysis of laminar profile for stimulation with 1 Hz frequency

Vertically the reverse of potential in layer IV of VCx can be observed (Fig. 4.5). Granular layer (always 4. subfigure) is characterized by the most diverse response to the stimulation within this group of animals. It can be noticed that first peak of response is stable whereas second peak is more varied.

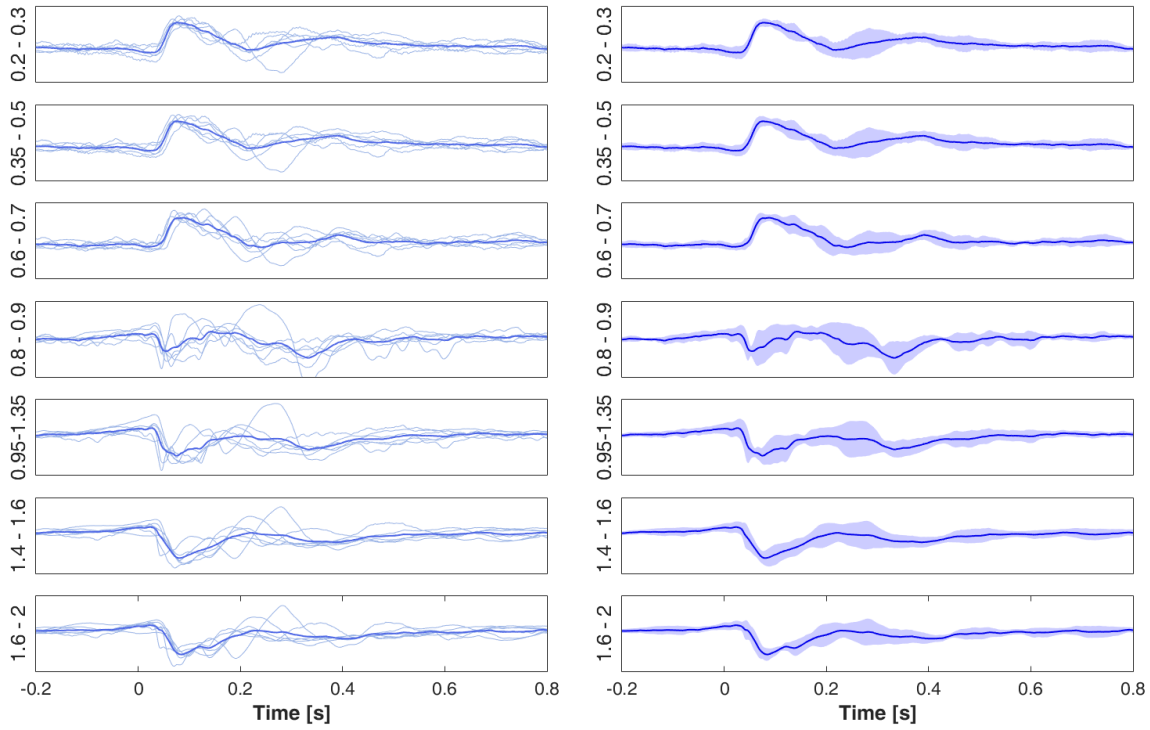

(a) (b)

Figure 4.5: Laminar profile in function of depth of the electrode for 1 Hz stimulation. All experiments averaged by 40 trials in time domain – bold line. Single animals are presented in two ways: by separated lines (4.5a) or by the standard deviation (4.5b). Point 0 s shows beginning of 5 s constant stimulation (here only 0.8 s is shown). Y axis is the same for both subfigures.

In the Figure 4.6 laminar profile of amplitude in dependence of depth of the electrode is shown. Amplitude of the first peak is very similar among animals and there is clear change of sign between third and forth channel (Fig. 4.6a). Amplitude of the second peak is characterized by a high variance and there is not difference between layers (Fig. 4.6b).

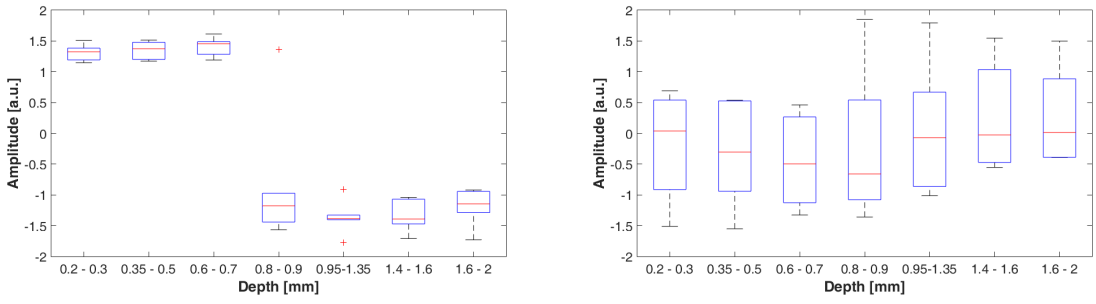

(a) Amplitude of the first peak. (b) Amplitude of the second peak.

Figure 4.6: Amplitude of the averaged signal in function of the depth of the electrode for stimulation of 1 Hz. On the left there is an amplitude of first peak (blue extremum in Fig. **??**), on the right – amplitude of second peak (red extremum in Fig. **??**). Blue section is a 95% confidence interval, red line is a mediana, red pluses are outliers.

In the Figure 4.7 laminar profile of amplitude of the peak fundamental and frequency and second harmonic in dependence of depth of the electrode is shown. Amplitude of the first peak is the biggest for fifth channel than for the others (Fig. 4.7a). Amplitude of the second peak is constant for all channels except the forth one. This channel also has the highest variance (Fig. 4.7b).

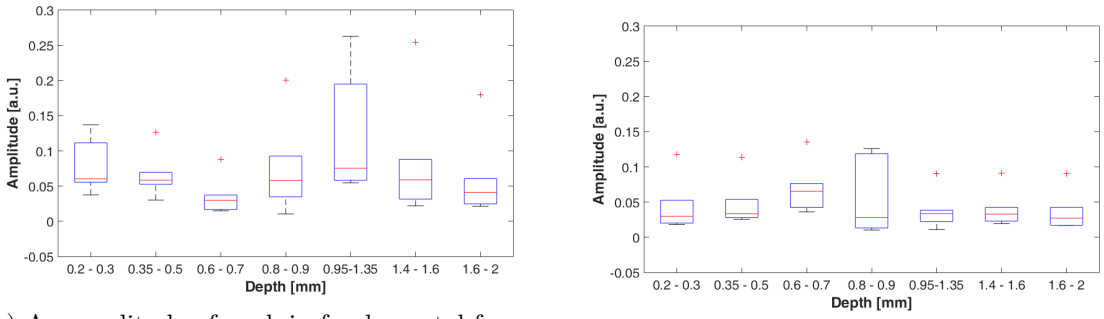

(a) An amplitude of peak in fundamental frequency.

(b) An amplitude of peak in the second harmonic.

Figure 4.7: Laminar profile of frequency domain in function of depth of the electrode for 1 Hz stimulation. On the left there is an amplitude of peak in fundamental frequency, on the right – amplitude of second harmonic. Blue section is a 95% confidence interval, red line is a mediana, red pluses are outliers.

4.5. Laminar analysis for stimulation with 2 Hz frequency

In the Figure 4.8 laminar profile of amplitude of response to stimulus in dependence of depth of the electrode for stimulation of 2 Hz is shown. Amplitude of the first peak is very similar among animals except channel 4 where variance is the biggest. (Fig. 4.8a). Tendency of amplitude of the second peak is like for 1 Hz: it has a high variance and there is not difference between layers (Fig. 4.8b).

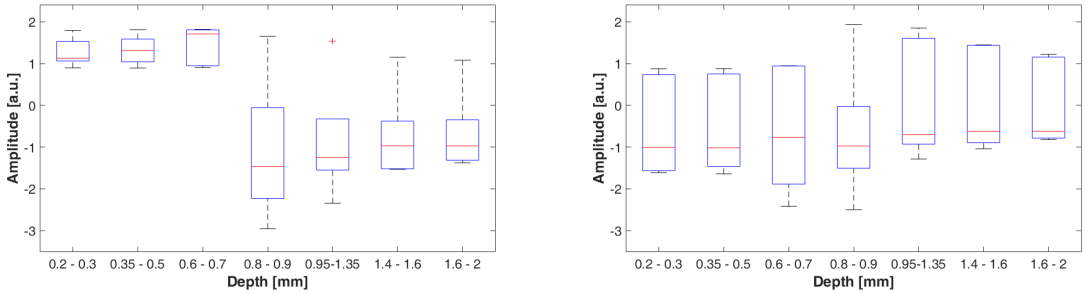

(a)

(b)

Figure 4.8: Laminar profile in function of depth of the electrode for 2 Hz stimulation.

In the Figure 4.9 laminar profile of amplitude of peak in 2 and 4 Hz in dependence of depth of the electrode for stimulation of 2 Hz is shown. There is no clear difference for amplitude of the first peak. (Fig. 4.9a). Median for second peak is the lowest for forth channel but all channels have the same, high variance (Fig. 4.9b).

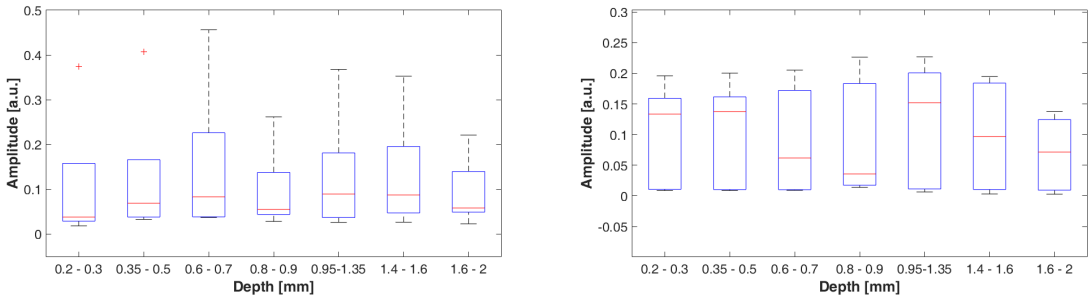

(a) (b)

Figure 4.9: Laminar profile in function of depth of the electrode for 2 Hz stimulation.

4.6. Laminar analysis for stimulation with 4 Hz frequency

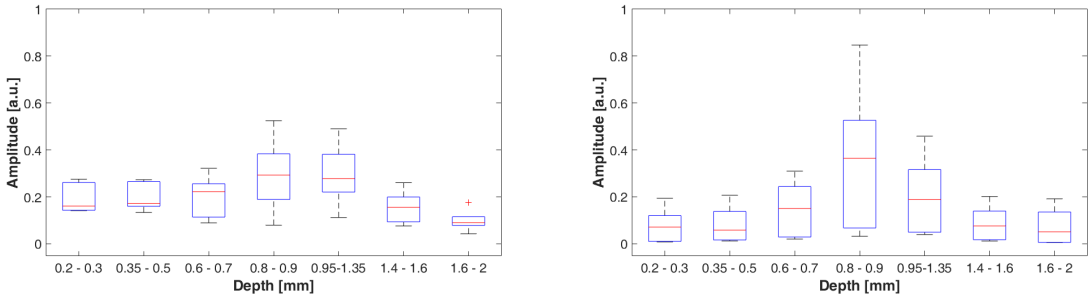

(a) (b)

Figure 4.10: Laminar profile in function of depth of the electrode for 4 Hz stimulation.

4.7. Laminar analysis for stimulation with 7 Hz frequency

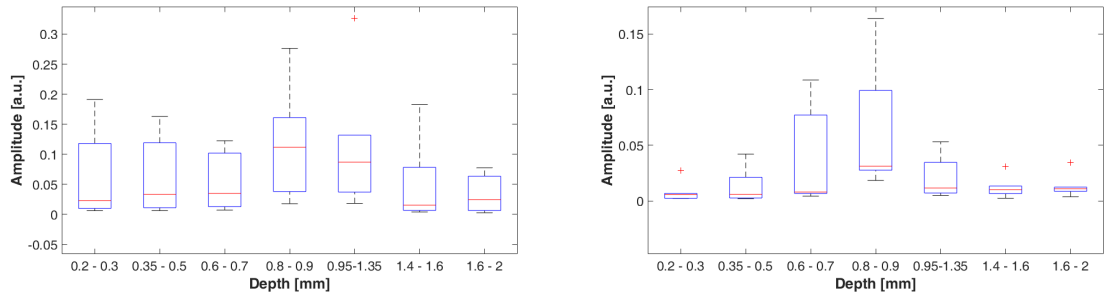

(a) (b)

Figure 4.11: Laminar profile in function of depth of the electrode for 7 Hz stimulation.

4.8. Laminar analysis for stimulation with 10 Hz frequency

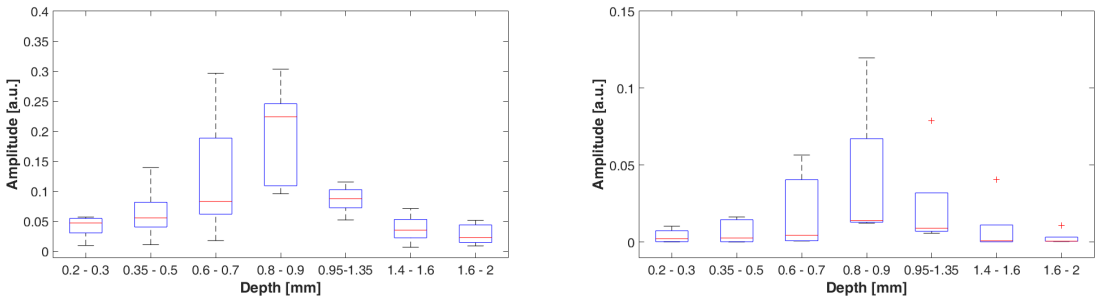

(a) (b)

Figure 4.12: Laminar profile in function of depth of the electrode for 10 Hz stimulation.

4.9. Laminar analysis for stimulation with 12 Hz frequency

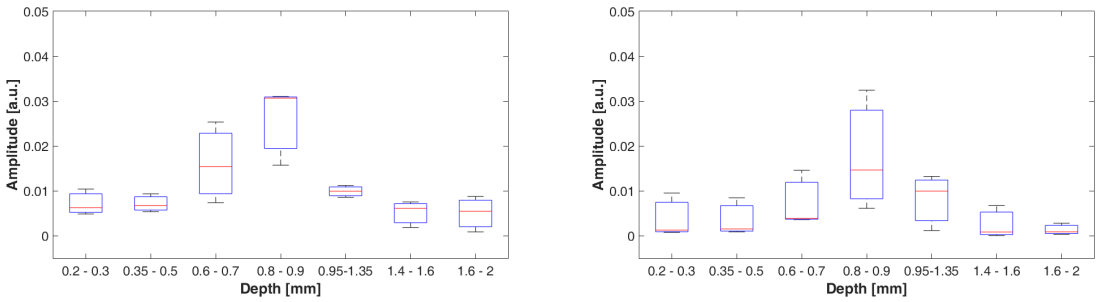

(a) (b)

Figure 4.13: Laminar profile in function of depth of the electrode for 12 Hz stimulation.

Chapter 5

Discussion

First of all, it is worth mentioning that even though all recordings were performed on the same structure, using the same electrode, brain anatomy differs between subjects. Individual channels were chosen for analysis based on the pattern of visual potential so there is no guarantee that one channel represents exactly the same structure for every animal. The same concerns the method of recording signal—local field potential is spatially an inaccurate method because it gathers signal from quite a big area of the brain, possibly spanning over multiple structures. On the other hand, this experiment was performed on a group of six animals and the obtained results are coherent and repeatable. Especially the latter confirms that the conclusions are correct.

Analysis of averaged signal for 1 Hz and 2 Hz indicates that there is a clear difference in amplitude of the first peak between supra- and infragranular layers. It can be a result of the fact that magnocellular channel enters from LGN mainly to layer IV of VCx and information from there propagates the further the bigger amplitude gets. For both stimulations there was a high variance of the amplitude of the second peak between animals, but there was no significant difference across the layers. Although the results of averaged potentials are similar for both low-frequency stimulations, there are substantial differences in the peaks for fundamental frequency and second harmonic. For 1 Hz stimulation channel 5 exhibited the highest amplitude and variance of fundamental frequency, while for 2 Hz stimulation channel 4 had the lowest value and variance. The same concerns second harmonic: for 1 Hz stimulation all channels had similar values except channel 4 which stood out having the highest variance. For 2 Hz stimulation the situation was quite opposite—channel 4 exhibited the lowest variance. Those contradictory effects may be a result of improper method of analysis. On the other hand, they could be due to high amplitude of low frequencies which are present in a sleeping animal so that low frequency of stimulation may be not enough to stand out (Wierzbicka et al., 2017).

For stimulation with frequency higher than 2 Hz the amplitude of peak in averaged signal was not calculated because stimulus occurred to often to generate full response and it was not possible to determine the peak. During analysis in the frequency domain the same tendency for all frequencies was observed. It is noticeable already for fundamental frequency, but for second harmonic it is much more apparent: channel 4 is characterized by the biggest amplitude and has lower variance than other channels. It also may be a cause of magnocellular entrance in layer IV in VCx. ...

Bibliography

Carlson (2013). *Physiology of behavior*. Pearson.

Maier, A. et al. (2010). "Distinct superficial and deep laminar domains of activity in the visual cortex during rest and stimulation". In: *Front Syst Neurosci* 4.

Paxinos, G. and C. Watson (2007). *The Rat Brain in Stereotaxic Coordinates*. sixth. Elsevier Inc.

Potworowski, J. et al. (2012). "Kernel current source density method". In: *Neural Comput* 24.2, pp. 541–575.

Schmolesky, M. (2007). "The Primary Visual Cortex". In: *Webvision: The Organization of the Retina and Visual System [Internet]*. Ed. by R. Nelson H. Kolb E. Fernandez. Salt Lake City (UT): University of Utah Health Sciences Center. URL: `https://www.ncbi.nlm.nih.gov/books/NBK11524/` (visited on 11/08/2017).

Stone, J. (1983). *Parallel Processing in the visual system*. New York: Plenum Press.

Thomson, A. M. (2010). "Neocortical layer 6, a review". In: *Front Neuroanat* 4, p. 13.

Waleszczyk, W. J., M. Bekisz, and A. Wrobel (2005). "Cortical modulation of neuronal activity in the cat's lateral geniculate and perigeniculate nuclei". In: *Exp. Neurol.* 196.1, pp. 54–72.

Welch, Peter D (1967). "The use of Fast Fourier Transform for the estimation of power spectra: A method based on time averaging over short, modified periodograms". In: *IEEE Trans. Audio and Electroacoust.* AU-15, pp. 70–73.

Wierzbicka, A. et al. (2017). "Analytical approaches to estimation of temporal frequency preference from visual evoked potentials". In: *Proc. of SPIE* 10445.104453W-1.

Wójcik, D. K. (2014). "Current Source Density (CSD) Analysis". In: *Encyclopedia of Computational Neuroscience*. Ed. by Jung R. Jaeger D. New York, NY: Springer.